



Modeling a Sodium Heat Pipe Experiment at SPHERE Using Sockeye

August 2025

Changing the World's Energy Future

Joshua E Hansel, Zachary Don Sellers, Jeremy Lee Hartvigsen, Piyush Sabharwall, Lise Charlot, Elia Merzari



DISCLAIMER

This information was prepared as an account of work sponsored by an agency of the U.S. Government. Neither the U.S. Government nor any agency thereof, nor any of their employees, makes any warranty, expressed or implied, or assumes any legal liability or responsibility for the accuracy, completeness, or usefulness, of any information, apparatus, product, or process disclosed, or represents that its use would not infringe privately owned rights. References herein to any specific commercial product, process, or service by trade name, trade mark, manufacturer, or otherwise, does not necessarily constitute or imply its endorsement, recommendation, or favoring by the U.S. Government or any agency thereof. The views and opinions of authors expressed herein do not necessarily state or reflect those of the U.S. Government or any agency thereof.

Modeling a Sodium Heat Pipe Experiment at SPHERE Using Sockeye

**Joshua E Hansel, Zachary Don Sellers, Jeremy Lee Hartvigsen, Piyush
Sabharwall, Lise Charlot, Elia Merzari**

August 2025

**Idaho National Laboratory
Idaho Falls, Idaho 83415**

<http://www.inl.gov>

**Prepared for the
U.S. Department of Energy
Under DOE Idaho Operations Office
Contract DE-AC07-05ID14517**

Modeling a Sodium Heat Pipe Experiment at SPHERE Using Sockeye

Joshua Hansel, Zachary Sellers, Jeremy Hartvigsen, Piyush Sabharwall, Lise Charlot

Idaho National Laboratory
1955 Fremont Ave, Idaho Falls, ID 83415
joshua.hansel@inl.gov; zachary.sellers@inl.gov; jeremy.hartvigsen@inl.gov;
piyush.sabharwall@inl.gov; lise.charlot@inl.gov

Elia Merzari

Department of Nuclear Engineering
The Pennsylvania State University
201 Old Main, University Park, PA 16802
ebm5351@psu.edu

ABSTRACT

The Single Primary Heat Extraction and Rejection Emulator (SPHERE) facility at Idaho National Laboratory was recently utilized to generate data for the startup and steady operation of a high-performance, sodium heat pipe over the course of 1,000 hours to test the detrimental, long-term effects of heat pipe operation. The setup consisted of a single, sodium heat pipe enclosed in a stainless-steel vacuum chamber, heated radiatively via a cylindrical ceramic-fiber heater configuration and cooled via a water-cooled calorimeter. Measurements included temperatures at several axial locations along the outer surface of the heat pipe, the power provided to the heaters, and the heat removal rate of the calorimeter. In this work, we use this data to validate heat pipe models in Sockeye, a heat pipe application based on the Multiphysics Object-Oriented Simulation Environment (MOOSE) framework. Sockeye provides various heat pipe models at an engineering scale appropriate for the multiphysics simulation of microreactors, which may feature several hundred heat pipes. This work details models of this experiment at SPHERE using various heat pipe models with Sockeye, including heat-conduction-based and compressible flow models of the heat pipe interior. Here, we also compare these models to the experimental data to assess the accuracy of several aspects of heat pipe modeling, including frozen startup, the effect of noncondensable gases, and the coupling of the heat pipe to its environment.

KEYWORDS

heat pipe; Sockeye; SPHERE; MOOSE

1. INTRODUCTION

Multiple microreactor designs are currently under development in the United States and may be ready to deploy within the next decade. These compact reactors will be small enough to be transported by truck and could help resolve certain energy challenges in several areas, from remote commercial and residential locations to military bases.

Microreactor designs vary, but most would be able to produce 1–50 MW of thermal energy either directly usable as heat or convertible to electric power. They can generate reliable electricity for commercial use or nonelectric applications, such as district heating, water desalination, and hydrogen fuel production.

One subset of microreactors is designed to transfer heat from the reactor via heat pipes, which were selected for their compact design, passive operation, and high thermal efficiency. Heat pipes have been used for several decades in a variety of applications, such as air conditioning, oil pipelines, electronics cooling, and space radiators [1, 2]; however, substantially less experience and data are available for high-temperature heat pipes, such as those proposed for microreactors.

The success and adoption of these microreactor designs depends on their safety characteristics and efficiency, both of which are tied to reactor core performance. It is important to demonstrate that a fuel design can operate reliably at high burnups, high power densities, and high coolant temperatures. The operational limitations involved, such as clad thermal creep, corrosion, and clad wastage formation, are all highly temperature-dependent phenomena. Consequently, an accurate prediction of temperature distributions during normal operation, as well as during transients, is key to demonstrating the safety of these designs. As a result, developers need validated tools and models to evaluate the passive safety features, design, and performance of microreactors.

The Multiphysics Object-Oriented Simulation Environment (MOOSE) is an open-source, finite-element framework upon which a variety of physics applications are built, including several that are highly relevant to microreactors [3, 4]. Most notable in this regard is DireWolf, a multiphysics code that couples neutronics, thermomechanics, and thermal hydraulics (see, for example, [5]).

One of the codes included in DireWolf is Sockeye, which was developed by the Nuclear Energy Advanced Modeling and Simulation Program and models the high-temperature heat pipes often used in microreactors. Heat pipes feature geometrically complex, porous wick structures, making it computationally intractable to generate a mesh of their interiors. The potential computational complexity is exacerbated by the need to use models of compressible and two-phase flows. Since it would be prohibitively expensive to use a high-fidelity model of each of the several hundred heat pipes in a microreactor core, Sockeye is designed for the engineering scale, employing one and two dimensional (1D and 2D) models. Sockeye offers three heat pipe models: a 1D, two-phase compressible flow model [6]; a 2D heat conduction model [7]; and the Liquid-Conduction, Vapor-Flow (LCVF) model, which is a 1D, single-phase compressible flow model for the vapor phase, coupled to a 2D heat conduction model for the liquid phase [8].

While heat pipes have been used for several decades, the experience and data on high-temperature heat pipes, such as those proposed for microreactors, are insufficient for design and analysis. The Single Primary Heat Extraction and Removal Emulator (SPHERE) facility at Idaho National Laboratory was designed to enable non-nuclear thermal and integrated systems testing of heat pipes under a range of operating conditions [9]. Several sodium heat pipe experiments have been performed at SPHERE since its opening, some of which have been utilized for Sockeye validation purposes [7]. Recently, researchers performed a long-duration heat pipe experiment [10], and the present work utilizes this experiment to validate Sockeye.

This paper outlines the work described in [11] and is outlined as follows. Section 2 describes the experimental setup at SPHERE, Section 3 describes the Sockeye models, Section 4 describes the experiment and model results, and Section 5 offers conclusions stemming from this work.

2. EXPERIMENTAL SETUP

This section describes the setup of SPHERE for its most recent experiments [10]. Figure 1 shows a photo of the assembly, exterior to the stainless-steel sanitary tube, which contains the heater, heat pipe, calorimeter, and insulation. The parameters of the sanitary tube are in Table 1. Thermal properties were computed from temperature-dependent correlations of stainless steel.

The sanitary tube is composed of five sections, which roughly correspond to the following list, starting at the condenser end (i.e., the left end in Figure 1):

1. Calorimeter fluid lines
2. Condenser
3. Adiabatic
4. Evaporator
5. Instrumentation leads.

The inner surface of the chamber is covered by a zirconia ceramic-fiber insulation blanket. The outer surface of the middle three chamber sections is insulated by a thin layer of Nomex aramid insulation to protect personnel from contact burns. A vacuum in the sanitary tube eliminates convective heat transfer, so solid regions separated by gaps transfer heat via radiation only.

Table 1. Sanitary tube parameters.

Parameter	Value
Material	Stainless steel
Emissivity	0.7
Outer diameter	12 in.
Thickness	0.134 in.



Figure 1. SPHERE setup.

Thermocouples are mounted via wire ties to the heat pipe surface at various axial positions. A fan blows air over the sanitary tube section containing the instrumentation leads to prevent overheating of the instrumentation leads, as the feedthrough wire that exits the sanitary tube is limited to 80°C.

The heating assembly is comprised of two semicylindrical ceramic-fiber heaters manufactured by Watlow [12]. The geometrical and material parameters of the heater are in Table 2.

Table 2. Heater parameters.

Parameter	Value
Material	Alumina-silica ceramic fiber
Density	200 kg/m ³
Specific heat capacity	1,000 J/(kg-K)
Thermal conductivity	0.15 W/(m-K)
Heated surface emissivity	0.9
Unheated surface emissivity	0.7
Total length	30 in.
Heated length	24 in.
Heat pipe heated length	22 in.
Inner diameter	6.5 in.
Outer diameter	10.5 in.
Heated thickness (estimated)	0.5 in.

The adiabatic section of the heat pipe is covered with a ceramic-fiber insulation blanket, the parameters of which are in Table 3. The thermal conductivity is linearly interpolated and extrapolated from the given points.

Table 3. Adiabatic section insulation parameters.

Parameter	Value
Material	Zirconia ceramic fiber
Density	8 lb/ft ³
Specific heat capacity	1,246 J/(kg-K)
Thermal conductivity	0.176 W/(m-K) at 800°C 0.22 W/(m-K) at 1000°C
Emissivity	0.7
Length	23.75 in.
Thickness	1 in.

The calorimeter is comprised of a stainless-steel coil surrounded by a stainless-steel shroud, the parameters of which are in Table 4. The thermal properties are computed from temperature-dependent correlations of stainless steel. Water at an inlet temperature of approximately 20°C enters the coil from the condenser end and flows toward the adiabatic section. The difference in temperature ΔT is measured, as is the water mass flow rate \dot{m} , allowing for the calorimeter heat removal rate $\dot{Q}_{\text{cal}}(t)$ to be computed as follows:

$$\dot{Q}_{\text{cal}}(t) = \dot{m}(t)c_p\Delta T(t), \quad (1)$$

where c_p is the specific heat capacity of water under these conditions.

The sodium heat pipe was manufactured by Advanced Cooling Technologies (ACT). Its internal specifications are proprietary and thus not listed in this paper. The heat pipe was not designed with noncondensable gases; however, we ran models with an assumed mass of 0.5 mg of air to investigate possible discrepancies with the measured data.

Table 4. Condenser section parameters.

Parameter	Value
Coil tube material	Stainless steel
Shroud material	Stainless steel
Emissivity	0.7
Length	30 in.
Coil tube outer diameter	0.375 in.
Coil tube wall thickness (assumed)	1 mm
Shroud outer diameter	6 in.

The experiment began at room temperature (approximately 20°C), with frozen sodium working fluid in the heat pipe. The power to the heater gradually increased, in steps, over the course of several hours, eventually reaching roughly 1,500 W at around 7.5 hours into the experiment. Then, the calorimeter pump turned on roughly 5.5 hours into the experiment. Up until that point, its fluid (water) was stationary in the coil tubes.

3. MODEL DESCRIPTION

We approximated the SPHERE assembly using the geometry shown in Figure 2, which also shows the axial locations of each thermocouple. Note that, because we believed the thermocouple located at the 51.5” position had fallen off the heat pipe and was thus measuring the temperature of the bottom of the vessel, it is omitted from the results.

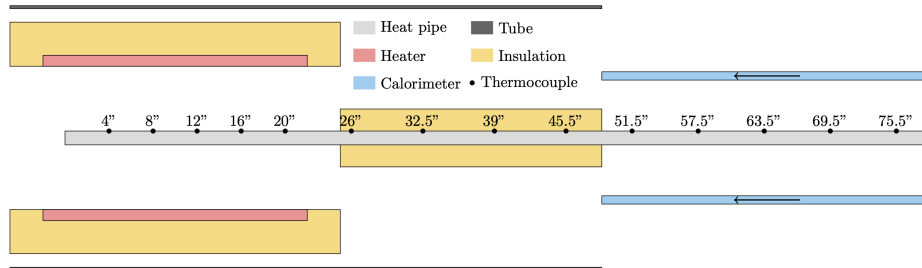


Figure 2. SPHERE model geometry diagram.

The experiment was approximated as a 2D axisymmetric problem, since the setup is relatively azimuthally uniform despite there being notable azimuthal dependencies, such as the structural supports that suspend the components along the axis of the sanitary tube.

The heater was modeled using a 2D heat structure, with a uniform volumetric heat source in the heated region of the heater assembly. The actual heater coils were embedded within the ceramic fiber and were approximated to reside within a 0.5-in.-thick region, starting at the inner surface, as shown in Figure 2. The adiabatic section insulation was also modeled using a 2D heat structure.

Radiative heat transfer was used to couple the various surfaces separated by a gap. The surfaces were assumed to be opaque, gray, and diffuse, and an infinite length approximation was applied, causing the surface elements to only be coupled to their radial neighbors at the same axial position. The resulting heat flux to surface i , q_i was computed as:

$$q_i(x, t) = \frac{\sigma [T_j(x, t)^4 - T_i(x, t)^4]}{\mathcal{R}_i}, \quad (2)$$

where σ is the Stefan–Boltzmann constant and T_i is the temperature of surface i . \mathcal{R}_i is the radiation resistance:

$$\mathcal{R}_i = \frac{1 - \epsilon_i}{\epsilon_i} + \frac{1}{F_{i,j}} + \frac{1 - \epsilon_j}{\epsilon_j} \frac{A_i}{A_j}, \quad (3)$$

where ϵ_i is the emissivity of surface i , $F_{i,j}$ is the view factor from surface i to surface j , and A_i is the area of surface i . For a two-surface enclosure, the enclosed surface i has a view factor of unity ($F_{i,j} = 1$). The other surface view factor $F_{j,i}$ may then be computed using the reciprocity rule.

The sanitary tube walls were included along the length of the heater block and the adiabatic section but not along the length of the condenser section, where all heat leaving the heat pipe surface was assumed to enter the calorimeter wall.

Radiation boundary conditions were applied to the outer surface of the sanitary tube. Equation (2) reduces to:

$$q(x, t) = \sigma \epsilon [T_\infty^4 - T(x, t)^4], \quad (4)$$

where T_∞ is the environmental temperature, assumed to be 20°C.

The calorimeter geometry was made complex by the coiled fluid line; therefore, the geometry was simplified to consist of a cylindrical shell sharing the same axis as the heat pipe, with the coolant fluid flowing in an annular cross section around the shell. The thickness of this annular channel was taken as the inner diameter of the coil tube so as to give approximately the same total volume. The calorimeter fluid was included in the model using a 1D, annular flow channel, with an inlet mass flow rate set as the experimentally measured mass flow rate $\dot{m}(t)$ and the outlet pressure set as 100 kPa. The calorimeter fluid was thermally coupled to the 2D inner calorimeter wall using a convection condition:

$$q(x, t) = h(T_{\text{fluid}}(x, t) - T_{\text{wall}}(x, t)). \quad (5)$$

The heat transfer coefficient h was determined by trial and error, due to the significant geometry approximations that invalidate the use of a specific correlation. The outer surface of the annular calorimeter fluid was assumed to be perfectly insulated.

The heat pipe was modeled using Sockeye's LCVF heat pipe model, where the vapor phase of the working fluid is modeled with 1D compressible flow and the liquid-filled wick and cladding are modeled with 2D heat conduction [8].

The 1D vapor flow channel in the LCVF model was discretized in space via the finite-volume method, and all 2D heat conduction regions were discretized via the Galerkin finite-element method. Table 5 gives the numbers of axial elements in each length. All 2D regions are modeled with three radial elements in each region. The BDF-2 scheme, which is second-order accurate, fully implicit, and A-stable, was used to discretize in time, and an adaptive time step size was employed that sought out a time step size such that the nonlinear solve converged in a given number of iterations, with the maximum time step size being 150 seconds.

Table 5. Numbers of axial elements.

Length Name	Number of Elements
Heater block unheated length (each)	3
Heated length overlapping with heat pipe	22
Heated length not overlapping with heat pipe	2
Adiabatic section	24
Condenser section	30

4. RESULTS

In this section, we present the results of the various models described in Section 3. The first 10 hours of the experiment were modeled, as this is the most interesting portion of the 1,000 hour experiment.

Before presenting the final results of this work, we discuss some intermediate results, based on various cooling models in the condenser section.

First, we considered a very simple cooling model, which used a uniform heat flux set to the experimentally measured heat removal rate. The results were clearly unphysical due to the inactive condenser section temperatures attaining temperatures below the environment temperature (room temperature, assumed to be 300 K). The uniform heat removal approximation fails to consider that very little heat is actually removed from the inactive length of the condenser, and it lacks any temperature feedback to keep temperatures physical. Thus we determined a nonuniform, temperature-dependent cooling model was essential for this problem.

Next, instead of applying a uniform heat flux, we applied a convection condition on the calorimeter wall, using the inlet calorimeter temperature as the reference temperature and using a heat transfer coefficient that was controlled to produce the experimentally estimated cooling rate. The results of this approach are shown in Figure 3. The system was predicted to continue heating up past when the experiment achieved a steady state, which suggests there are additional heat losses in the system not being captured in the model. For example, possible heat losses could be due to radiation escaping the calorimeter or from underestimating the evaporator and adiabatic section losses.

At this point, we must note that we believed the evaporator thermocouples carried a significant amount of error. Upon observing the significant temperature differences between the evaporator and adiabatic section, we suspected issues, as isothermal performance had been achieved at lower operating temperatures by ACT. After some discussion with ACT, we believed the cause of the issues was that the thermocouples were wire-tied to the heat pipe instead of tack-welded. Wire-tying can introduce a significant amount of thermal resistance. Additionally, with the thermocouples being directly heated by radiation, they can read much higher than the surface to which they are attached. Similar arguments can be made for temperatures being measured too low in the cooled sections. The adiabatic section is potentially the most trustworthy region, as little heat loss should occur there.

Since we found that directly applying the experimentally estimated calorimeter power for the cooling condition led to an underestimation of losses, the next approach accepted that additional unaccounted for heat losses were present and artificially increased the heat transfer coefficient in response. Through trial and error, the value $h = 35 \text{ W}/(\text{m}^2\text{-K})$ matched up with the data decently well. The results are shown in Figure 4. The condenser temperatures have a very

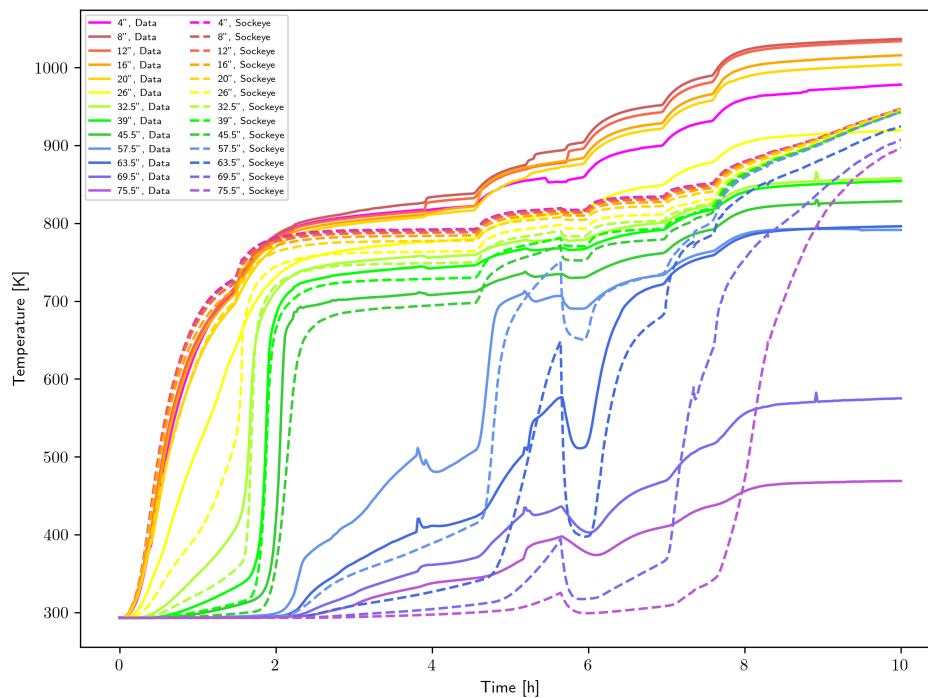


Figure 3. Temperature transient comparison between Sockeye and the experimental data using the controlled heat transfer coefficient cooling model.

delayed rise, but the final temperatures do not falsely converge to each other as they do in Figure 3.

Finally, we applied the cooling model described in Section 3. This is the most mechanistic of the options and offers an advantage over the previously described cooling model in that the coolant fluid temperature can now vary from the inlet temperature. The results are shown in Figure 5. Since the calorimeter fluid was not fixed at the inlet temperature, the condenser section temperatures could increase much earlier and end up at hotter values. As this is considered the best set of models applied to this experiment, we examined some additional plots to understand what was happening in the system. The final temperature distribution is shown in Figure 6. The experimental data reflect a noticeable peak in the evaporator section, but for the time being, we assumed this largely stemmed from measurement error. The adiabatic and condenser sections saw decent, though still not excellent, matches between the data and Sockeye results. The vertical line “Inactive start” denotes the start of the inactive length of the heat pipe, which is composed of two components: the excess working fluid pool and the noncondensable gas pool. Figure 7 shows each of the inactive lengths as a function of time. The “Unstarted” curve corresponds to a startup front model in the LCVF model, which marks the transition between rarefied gas flow and continuum flow. This was mainly active for the first hour, after which it simply followed the “Condenser pool plus NCG” curve. The noncondensable gas pool started out very large, when the partial pressure of the working fluid was small but shrunk significantly with increasing temperature and system pressure. The condenser pool length was roughly a few inches and then grew as the system continued to heat up due to the thermal expansion of the working fluid.

The power transient is shown in Figure 8. The cooling power in Sockeye significantly exceeds the cooling power measured in the experiment, which was necessary to reproduce the approach to steady-state conditions. This approach also captures some of the peak associated with the

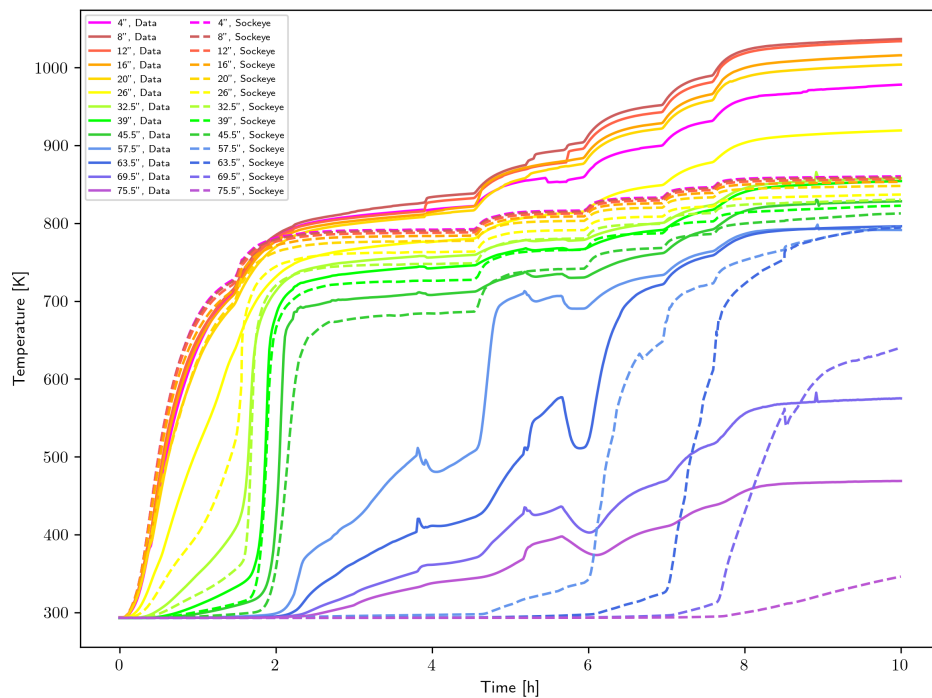


Figure 4. Temperature transient comparison between Sockeye and the experimental data using the specified heat transfer coefficient cooling model.

onset of calorimeter flow. The sets are described as follows:

- “Heater, Data”: The heater input electrical power.
- “Cooler, Data”: The experimental calorimeter power estimated via Equation (1).
- “Sonic Limit”: The sonic operational heat pipe limit, estimated via an analytic relation at the current evaporator end vapor temperature in Sockeye.
- “Capillary Limit”: The capillary operational heat pipe limit, estimated via an analytic relation at the current evaporator end vapor temperature in Sockeye.
- “Heater, Sockeye”: The heater input power applied in Sockeye, which is interpolated from the experimental data.
- “HP Heat Rate, Sockeye”: The heat rate across the evaporator-adiabatic interface in the vapor core in the heat pipe, which is used in comparison against the analytic limits in Sockeye.
- “Evap. Radial Loss, Sockeye”: The heat loss rate through the outer system boundaries in the evaporator section in Sockeye.
- “Evap. End Loss, Sockeye”: The heat loss rate through the axial, evaporator end of the heating block in Sockeye.
- “Adia. Loss, Sockeye”: The heat loss rate through the outer system boundaries in the adiabatic section in Sockeye.
- “Cooler, Sockeye”: The heat loss rate through the calorimeter section in Sockeye.

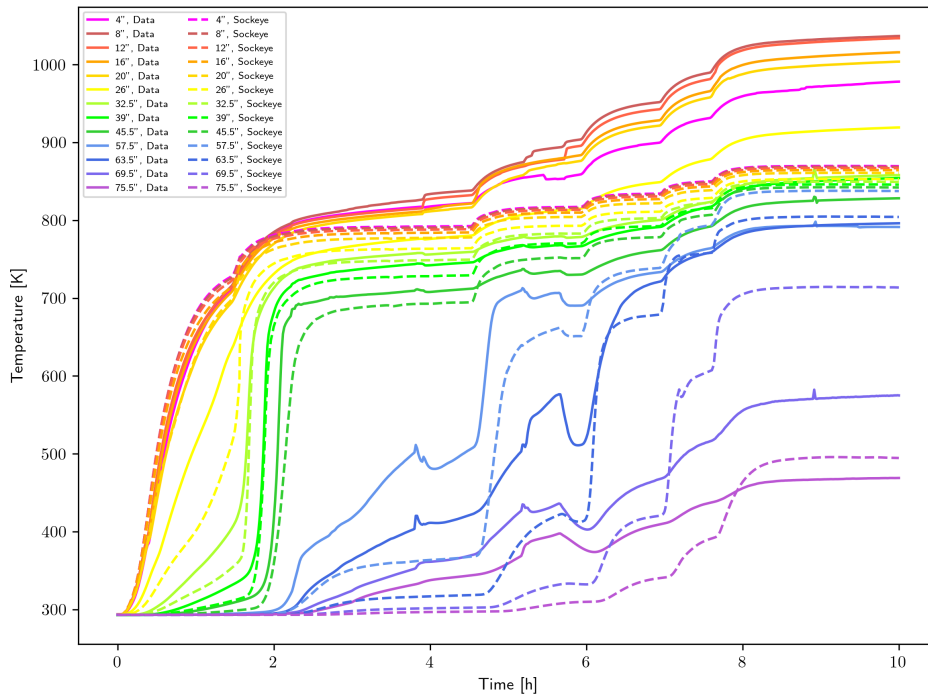


Figure 5. Temperature transient comparison between Sockeye and the experimental data using the flow cooling model.

- “Total Losses, Sockeye”: The sum of all heat losses in Sockeye, which at steady state should match “Heater, Sockeye.”

By comparing “HP Heat Rate, Sockeye” to the limit curves, we predicted that the heat pipe would only be limited during the first hour of the experiment. Roughly 60% of the heater power is lost through the evaporator boundary. Much less is lost through the adiabatic section boundary.

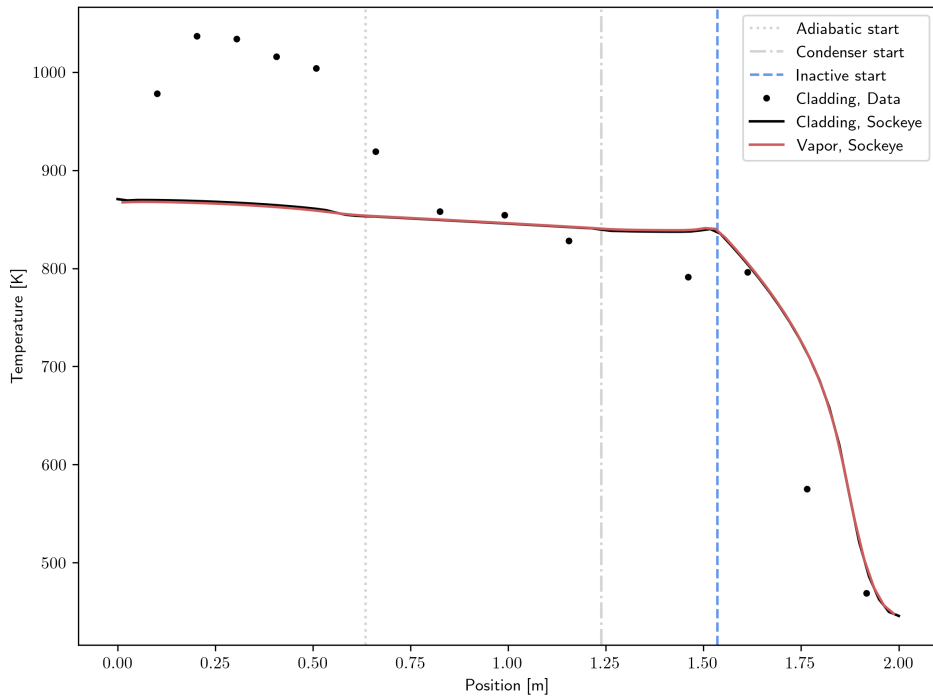


Figure 6. Final temperature profile comparison between Sockeye and the experimental data using the flow cooling model.

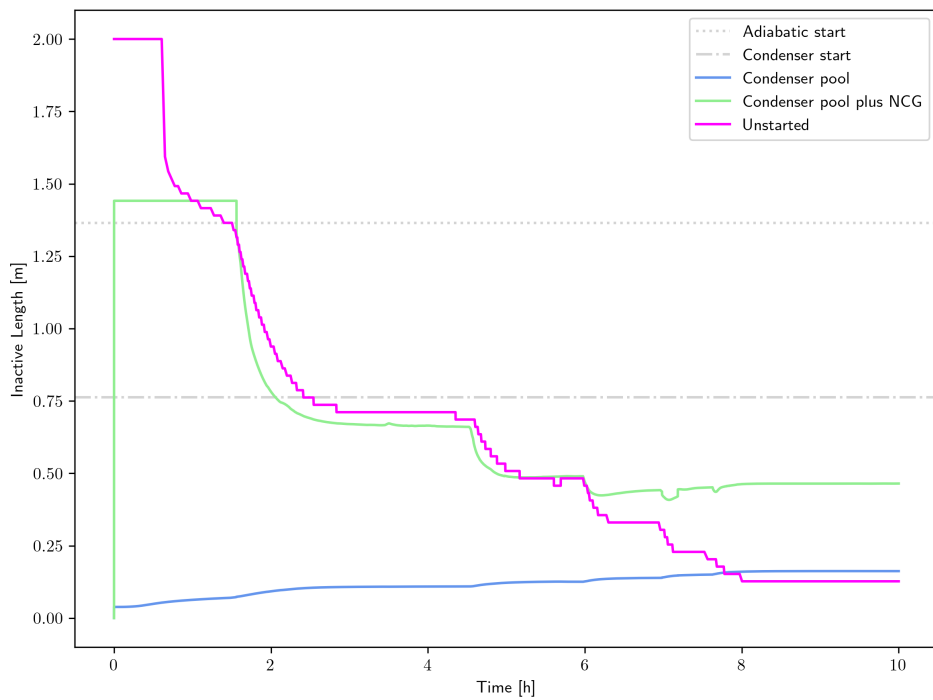


Figure 7. Inactive-length transient comparison between Sockeye and the experimental data using the flow cooling model.

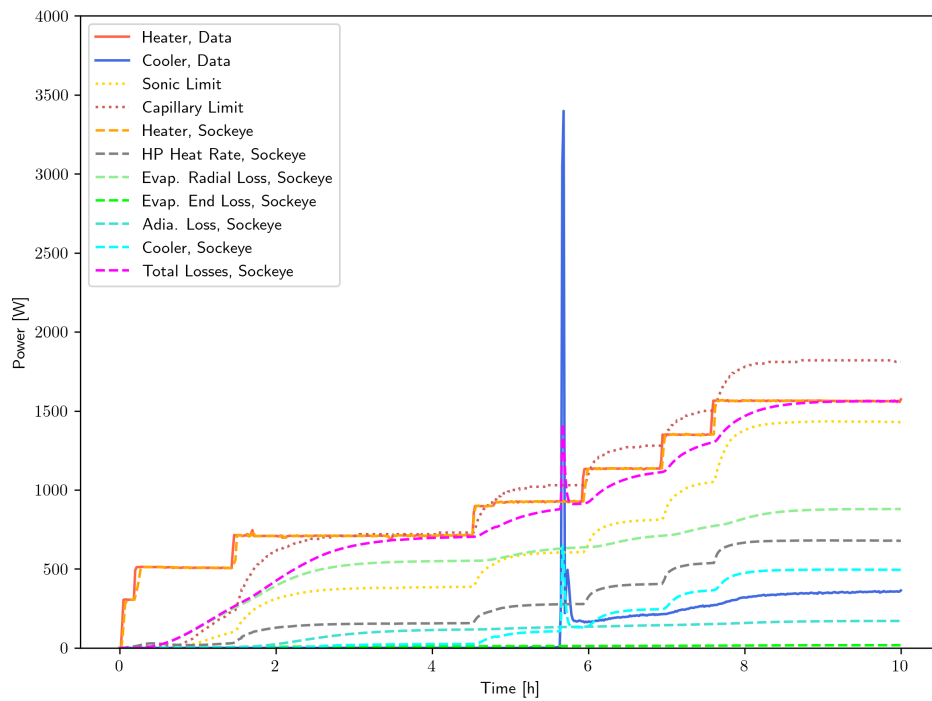


Figure 8. Power transient comparison between Sockeye and the experimental data using the flow cooling model.

5. CONCLUSIONS

We used the recent long-duration sodium heat pipe experiment at SPHERE to validate the Nuclear Energy Advanced Modeling and Simulation heat pipe code Sockeye. The first 10 hours of this experiment involved the startup of the heat pipe from a frozen state, which is a challenging regime to model due to the low pressure and temperature inside the heat pipe. We created several models of the experiment, including different heat pipe models and different cooling models. The calorimeter, which consisted of a tube coiled around the heat pipe axis, was greatly approximated due to its geometrical complexity to avoid the need for a 3D model. The most complex approximation of the calorimeter, in which the cooling fluid was modeled with a 1D flow channel, proved the most accurate of the considered cooling models. When the experimentally estimated calorimeter power was used directly, we believed the cooling was underestimated and the resulting simulation predicts much hotter heat pipe temperatures. With the best model of the experiment, the transient was decently matched by Sockeye. The condenser temperature values were much lower than in the adiabatic section, suggesting the possibility of effects such as a pooling of excess working fluid and the presence of noncondensable gases. In addition to the challenges faced by simplifying the geometry, other challenges arose due to uncertainty in important physical properties such as thermal conductivity and emissivity—to which results are quite sensitive. Furthermore, we believed the thermocouple measurements in the experiment, particularly those in the evaporator section, had significant error as a result of wire-tying the thermocouples to the heat pipe instead of welding them to it. In response to the difficulties encountered in this validation exercise, the Sockeye team is working with the SPHERE team to improve future experiments. The SPHERE team is currently rebuilding the experimental setup used in this work to address possible thermocouple error, so new experimental data may be available in early 2025.

ACKNOWLEDGMENTS

We would like to thank Jeffrey Diebold and Calin Tarau of ACT for lending their expertise on heat pipe operation, interpreting SPHERE data, and offering experimental advice.

This work was funded by the Office of Nuclear Energy of the U.S. Department of Energy, through the Nuclear Energy Advanced Modeling and Simulation program, under contract no. DE-NE0008983. Sockeye development is being carried out under the auspices of Idaho National Laboratory, a contractor of the U.S. Government, under contract no. DEAC07-05ID14517. Accordingly, the U.S. Government retains a nonexclusive, royalty-free license to publish or reproduce the published form of this contribution, or allows others to do so, for U.S. Government purposes.

REFERENCES

- [1] A. Faghri, *Heat Pipe Science and Technology*. Global Digital Press, second ed., 2016.
- [2] D. A. Reay, P. A. Kew, and R. J. McGlen, *Heat Pipes: Theory, Design and Applications*. Elsevier Ltd., sixth ed., 2014.
- [3] G. Giudicelli, A. Lindsay, L. Harbour, C. Icenhour, M. Li, J. E. Hansel, P. German, P. Behne, O. Marin, R. H. Stogner, *et al.*, “3.0-moose: Enabling massively parallel multi-physics simulations,” *SoftwareX*, vol. 26, p. 101690, 2024.
- [4] R. Martineau, D. Andrs, R. Carlsen, D. Gaston, J. Hansel, F. Kong, A. Lindsay, C. Permann, A. Slaughter, E. Merzari, R. Hu, A. Novak, and R. Slaybaugh, “Multiphysics for

- nuclear energy applications using a cohesive computational framework,” *Nuclear Engineering and Design*, vol. 367, p. 110751, 2020.
- [5] C. Matthews, V. Laboure, M. DeHart, J. Hansel, D. Andrs, Y. Wang, J. Ortensi, and R. C. Martineau, “Coupled multiphysics simulations of heat pipe microreactors using DireWolf,” *Nuclear Technology*, vol. 207, no. 7, pp. 1142–1162, 2021.
- [6] J. E. Hansel, R. A. Berry, D. Andrs, M. S. Kunick, and R. C. Martineau, “Sockeye: A one-dimensional, two-phase, compressible flow heat pipe application,” *Nuclear Technology*, vol. 207, no. 7, pp. 1096–1117, 2021.
- [7] J. Hansel, J. Hartvigsen, P. Sabharwall, L. Ibarra, and B. Feng, “Sockeye validation support using the SPHERE facility,” in *International Conference on Physics of Reactors (PHYSOR)*, (Pittsburgh, PA), American Nuclear Society, May 2022.
- [8] J. E. Hansel, C. da Silva Bourdot Dutra, L. Charlot, and E. Merzari, “The liquid-conduction, vapor-flow heat pipe model in sockeye,” *Nuclear Engineering and Design*, vol. 426, p. 113359, 2024.
- [9] P. Sabharwall, J. Hartvigsen, T. Morton, Z. Sellers, and J. S. Yoo, “SPHERE assembly and operation demonstration,” Tech. Rep. INL/EXT-20-60782, Idaho National Laboratory, December 2020.
- [10] Z. D. Sellers, T. Neumann, J. Hartvigsen, and P. Sabharwall, “Single primary heat extraction and removal emulator (SPHERE) long duration testing,” Tech. Rep. INL/RPT-24-05019, Idaho National Laboratory, 2024.
- [11] J. E. Hansel, V. Kyriakopoulos, and L. Charlot, “Leveraging MARVEL and SPHERE to demonstrate NEAMS thermal hydraulics codes,” Tech. Rep. INL/RPT-25-82868, Idaho National Laboratory, January 2025.
- [12] “Ceramic fiber heaters.” <https://www.watlow.com/products/heaters/high-temperature-heaters/ceramic-fiber-heaters>. Accessed: 2024-12-11.